Numerical study for traveling waves in directional solidification

Herbert Levine and Wouter-Jan Rappel
Department of Physics and Institute for Nonlinear Science, University of California, San Diego, La Jolla, California 93093
(Received 30 April 1990)

A recent experiment on the directional solidification of liquid crystals has exhibited traveling waves. In this Brief Report we present numerically obtained solutions for these traveling waves by generalizing the methods previously employed to look for steady-state patterns. The results agree with our earlier predictions based on a stability analysis and complete the bifurcation diagram for the system at hand.

Recently, Simon, Bechhoefer, and Libchaber[1] have reported various new instabilities in the directional solidification of liquid crystal. Among other things, they observed solitary inclusions which propagate through the stationary cellular pattern. In fact, these traveling-wave-like patterns have been observed in eutectic solidification,[2] convection cells,[3] and other systems as well.

Coullet *et al.*[4] have provided a natural explanation for these propagating inclusions. Crucial to their argument is the existence of a parity-breaking bifurcation which breaks the reflection symmetry of the original steady-state pattern, and thereby gives rise to traveling wave states. In the case where such a bifurcation is subcritical, kinks connecting the reflection symmetric with the asymmetric state can arise. The resulting kink-antikink pair exhibits all the qualitative features of the experimentally discovered inclusion.

Riecke and we[5] have explained the observed states from a different point of view. Near the codimension two point, i.e., where both the q and $2q$ modes become unstable, one can write the following set of amplitude equations for the amplitudes for the q mode (z_1) and the $2q$ mode (z_2) (the ellipsis stand for higher-order terms):

$$\dot{z}_1=\alpha z_1+c_1 z_1^* z_2+a_1 z_1|z_1|^2+b_1 z_1|z_2|^2+\cdots , \quad (1)$$

$$\dot{z}_2=\beta z_2+c_2 z_1^2+a_2 z_2|z_1|^2+b_2 z_2|z_2|^2+\cdots . \quad (2)$$

The pattern (interface position) z is given in terms of the complex amplitudes z_1 and z_2 by $z=z_1 e^{iq_{ct}x}+z_2 e^{2iq_{ct}x}+\text{c.c.}+\cdots$, and the coefficients appearing in these equations are related to the control parameter v and the wave number q.

In Ref. 5 we have discussed in detail the bifurcation diagrams resulting from Eqs. (1) and (2). These bifurcation diagrams exhibit all the experimentally observed states and explain quite naturally the traveling-wave state. We also presented numerically obtained solutions for the three steady-state branches: We found two "mixed" modes, i.e., states with both z_1 and z_2 nonzero (which we called S_- and S_+), and a pure period-doubled solution S_2, with only z_2. We argued there that the traveling-wave branch would start at exactly the location of the parity-breaking instability, which was subsequently found numerically, using the methodology of Ref. 6. In this paper we complete this picture by presenting an explicit calculation of the (finite-amplitude) traveling-wave states that occur in this system.

Let us first describe the basic equations of directional solidification[7] in the presence of a nonzero velocity in the transverse (x) direction. We assume that the alloy is characterized by the standard phase diagram (see, for example, Kessler and Levine[8]). In both the liquid and the solid phase (for the liquid-crystal case this is the nematic and isotropic case), the concentration field obeys the diffusion equation

$$D_\alpha \nabla^2 c=\frac{\partial c}{\partial t} , \quad (3)$$

where D_α is the diffusion constant in the liquid or the solid. The concentration far away from the interface, c_∞, is fixed for each experiment. Local thermodynamic equilibrium requires that the temperature is the same on both the liquid and the solid sides of the interface. From the phase diagram we have

$$T_S=\hat{T}_M-c_S m_S, \quad T_L=\hat{T}_M-c_L m_L ,$$

where m_s (m_l) and c_s (c_l) are, respectively, the slope dT/dc in the solid (liquid) phase and the concentration on the solid (liquid) sides of the interface. $\hat{T}_M$ is the melting temperature for the pure material ($c=0$) and has a Gibbs-Thomson shift due to the curvature κ: $\hat{T}_M=T_M(1-d_0\kappa)$, where the capillary length d_0 can be expressed in terms of the surface energy σ and the latent heat L: $d_0=\sigma/L$. Here we have neglected any possible dependence of d_0 on the angle between the interface normal and the crystal axes.

The final boundary condition follows from the conservation of matter,

$$-v_n(c_L-c_S)=D_L(\hat{\mathbf{n}}\cdot\nabla c)_L-D_S(\hat{\mathbf{n}}\cdot\nabla c)_S , \quad (4)$$

where v_n is the normal velocity: $v_n=(v_x^2+v_y^2)^{1/2}$. In the case of a directional solidification experiment the temperature is imposed externally. For convenience let us choose

$$T(y)=T_M+G_y , \quad (5)$$

so that at $y=0$ we have $T=T_M$.

To cast the equations in their final form, we go to the moving frame, moving with velocity $\mathbf{v}=(v_x,v_y)$, rescale c by c_∞, and rescale the lengths by the diffusion length $v_y/2D_L$. Then the equations read

$$\begin{aligned}
&\nabla^2 c+\frac{2D_L}{v_y}\mathbf{v}\cdot\nabla c=0 \quad \text{(liquid)}\,,\\
&\alpha\nabla^2 c+\frac{2D_L}{v_y}\mathbf{v}\cdot\nabla c=0 \quad \text{(solid)}\,,\\
&(\hat{\mathbf{n}}\cdot\nabla c)_L-\alpha(\hat{\mathbf{n}}\cdot\nabla c)_S=-2(1-k)c_L\hat{n}_y\,,\\
&c_L=\frac{c_S}{k}=\frac{-y}{\xi}-\gamma\kappa\,,
\end{aligned} \tag{6}$$

where $k=m_L/m_S$, $\alpha=D_S/D_L$, $\gamma=\upsilon d_0 T_M/2D_L m_L c_\infty$, and $\xi=\upsilon m_L c_\infty/2D_L G$.

To derive the integro-differential equation, let c_l be equal to c everywhere in the liquid and zero in the solid. Let c_s be the same with the solid and liquid reversed.

TABLE I. Parameter values of the liquid-crystal system used in the numerical calculation.

d_0	$=2\times10^{-8}$ cm
G	$=23.3$ K/cm
T_M	$=313.65$ K
m_l	$=1$°/mol %
c_∞	$=1.2$ mol %
D_l	$=3.8\times10^{-6}$ cm/s^2
D_s	$=D_l$
k	$=0.88$

From Eqs. (6) and the boundary condition $c\to1$ at ∞, we can write

$$\begin{aligned}
c_l&=1+\int c_L\hat{\mathbf{n}}'\cdot\nabla' G_L-\int G_L\phi_1\,,\\
c_s&=\int c_S\alpha\hat{\mathbf{n}}'\cdot\nabla G_S-\int G_S\phi_2\,,
\end{aligned} \tag{7}$$

where the liquid-phase Green's function is

$$G_L=\sum_n\frac{1}{4p}e^{-p(y-y')-(v_x/2)(x-x'+2n)}K_0((p^2+v_x^2/4)^{1/2}[(x-x'+2n)^2+(y-y')^2]^{1/2})\,, \tag{8}$$

and there is an analogous expression for G_S. Note that p, the Peclet number, is defined solely with the $\hat{\mathbf{y}}$ velocity: $p=v_y\lambda/4D_L$. Throughout this paper we take $\alpha=1$, for which Eqs. (7) reduce to the single equation

$$c_s=1+\int(1-k)(-y/\xi-\gamma\kappa)(\hat{\mathbf{n}}'\cdot\nabla' G)\,ds'\,. \tag{9}$$

The computational procedure consists of parametrizing the (unknown) boundary ($x=0$ to $x=\lambda$) with $2N$ points of equal arclength separation. As our independent variables we take the normal angle $\hat{\mathbf{n}}\cdot\hat{\mathbf{y}}=\cos\theta$ defined on the midpoints of the sections of equal arclength. The additional independent variables are the position of the cell,

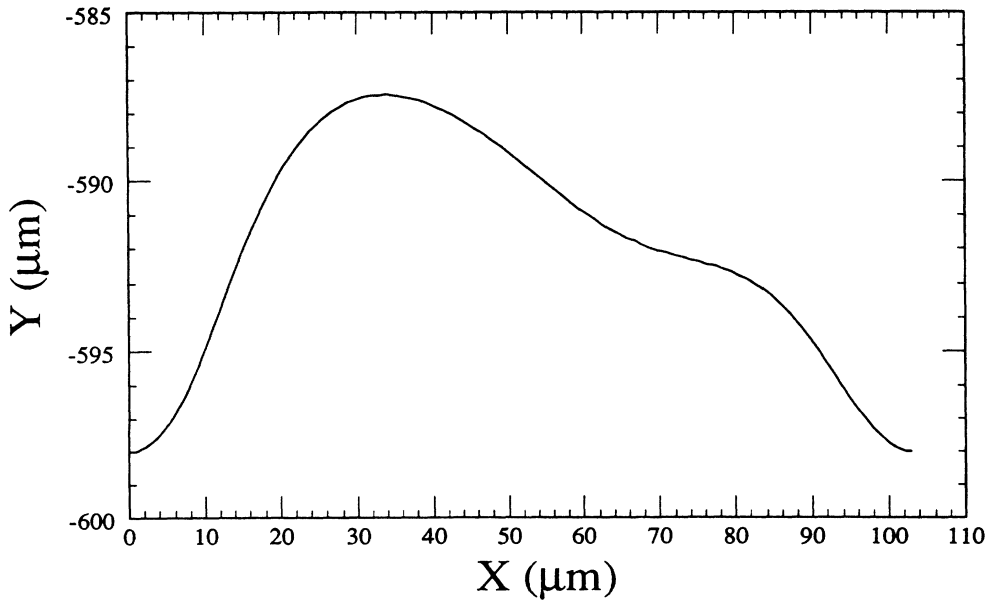

FIG. 1. A typical traveling-wave pattern.

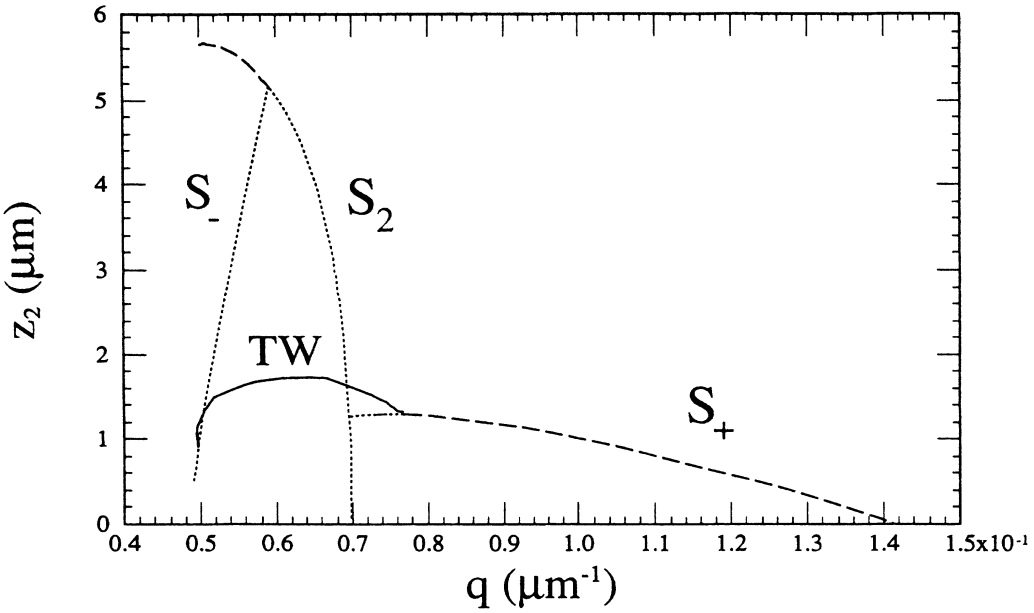

FIG. 2. The numerically obtained bifurcation diagram, with the steady-state branches S_+, S_-, and S_2, and the traveling-wave (TW) branch. z_2 is the amplitude of the $2q$ mode. Stable branches are represented by dashed lines and unstable branches by dotted lines.

y_0, and the velocity in the x direction, v_x. Therefore, we need $2N+1$ equations to describe the system. We have $2(N-1)$ equations from the integral equations on the points of equal arclength excepting the interval endpoints. In addition, we require that the position to the endpoints are equal, i.e., $y(0)=y(N)$, and that the slope vanishes at both the tip and the tail.

It is worth pointing out that an explanation as to why a parity-breaking bifurcation gives rise to a traveling wave can be given in a natural way if we consider the counting of variables and equations. The basic point is that translation invariance in the $\hat{\mathbf{x}}$ direction must be broken by the computational procedure, so as to be searching for a unique solution. This has been done above by demanding that the slopes at the endpoint not only be continuous but also equal to zero This leaves us with one more equation than variables, and hence necessitates the introduction of the velocity in the x direction as an extra unknown.

The resulting $2N+1$ nonlinear equations were iterated by using Newton's algorithm, following the procedure discussed in Ref. 8. In our program we used the CLAMS routine DNSQE with an absolute accuracy of 10^{-5}. The number of discretization points used was 50. We applied this methodology to a system with material parameters given in Table I. These are mostly based on the actual experiment of Simon *et al.*, with the exception of the use of a larger diffusion constant. This should not have a major qualitative effect on any of the results reported here.

In Fig. 1, we show a typical traveling-wave pattern with, in this case, a nonzero velocity in the negative x direction. In fact, there exists a simple check of our program since the result should be antisymmetric under reversing the velocity. Indeed, we have found a solution with the same velocity, but now in the positive x direction, which is the reflection of Fig. 1 about its endpoint.

Figure 2 shows a complete branch of traveling waves for the system described in Table I. We have plotted the amplitude of the $2q$ mode z_2 versus the wave number q. In addition to the already-found steady-state solutions S_-, S_+, and S_2,[5] we are now able to connect the steady-state branches with a traveling-wave branch. This bifurcation diagram is in agreement with our earlier work. There we predicted the existence of a traveling wave arising from a stability analysis. The velocities for which the traveling wave bifurcates off the steady-state branches S_- and S_+ correspond exactly with the predicted values. Note that the traveling-wave branch turns around before it merges with the S_- branch. However, since the S_- branch is unstable, this is in some sense unphysical. The branch does not turn around when it merges with the S_+ branch indicating a *supercritical* bifurcation.

In summary, we have explicitly found the existence of traveling waves in directional solidification. The points at which these states appear are correctly predicted by the stability analysis of Ref. 5. This fact enabled us to efficiently find these nonlinear patterns in (enormous) parameter space.

[1]A. Simon, J. Bechhoefer, and A. Libchaber, Phys. Rev. Lett. **61**, 2574 (1988).
[2]M. Rabaud, S. Michalland, and Y. Couder (unpublished).
[3]G. Faivre, S. de Cheveigne, C. Guthmann, and P. Kurowski, Europhys. Lett. **9**, 779 (1989).
[4]P. Coullet, R. E. Goldstein, and G. H. Gunratne, Phys. Rev. Lett. **63**, 1954 (1989).
[5]H. Levine, W.-J. Rappel, and H. Riecke, Phys. Rev. A (to be published).
[6]D. Kessler and H. Levine, Phys. Rev. A **41**, 3197 (1990).
[7]For a review, see, e.g., D. A. Kessler, J. Koplik, and H. Levine, Adv. Phys. **37**, 255 (1988); J. Langer, in *Chance and Matter,* edited by J. Souletie, J. Vannimenus, and R. Stora (North-Holland, Amsterdam, 1987).
[8]D. Kessler and H. Levine, Phys. Rev. A **39**, 3041 (1989).